RAPID COMMUNICATIONS

PHYSICAL REVIEW B VOLUME 30, NUMBER 12 15 DECEMBER 1984

Image-potential and intrinsic surface states on Ag(100)

B. Reihl, K. H. Frank, and R. R. Schlittler
IBM Zurich Research Laboratory, 8803 Rüschlikon, Switzerland
(Received 30 July 1984)

Applying $\vec{k}$-resolved inverse photoemission spectroscopy to the Ag(100) surface, we have found two different types of unoccupied electronic surface states: (i) Near-normal-incidence, image-potential surface states produce a steplike spectral feature about 0.5 eV below the vacuum level; (ii) near the $\bar{X}$ point of the surface Brillouin zone, an *s*-like Shockley-type surface state appears at $E_F+3.8$ eV, in agreement with electroreflectance measurements by Kolb *et al.* Both surface states are quenched by the adsorption of water at 110 K.

Recently, the first unoccupied intrinsic surface state (SS) on a metal surface was discovered on Ag(110) by using $\vec{k}$-resolved inverse photoemission spectroscopy (KRIPES).[1] Furthermore, the seemingly general existence of a spectral feature near the vacuum level E_{vac} in the KRIPES data of Ni(100) (Ref. 2) and Cu(100) (Refs. 2 and 3) was recently proven[4,5] to arise from image-potential surface states. The latter states are not intrinsic, neither do they *a priori* reveal a material property. They are existent on surfaces which have a band gap around E_{vac} in the projected bulk-band structure. Accordingly, electron-energy-loss spectroscopy (EELS) and LEED-beam (LEED denotes low-energy electron diffraction) intensity measurements have given evidence for the existence of these universal types of surface states.[6] Contrarily, intrinsic surface states, although also bound to a projected bulk-band gap at the surface, are a material property. As first discussed by Shockley[7] they are split off from bulk bands owing to the jump of the electrostatic potential at the surface. They may play a decisive role in chemical processes occurring at the surface-vacuum interface, and determine its bonding and catalytic properties. In contrast to the image-potential SS's, they may be occupied as well as unoccupied, and numerous occupied intrinsic SS's on many single-crystal surfaces have been observed mostly by angle-resolved photoelectron spectroscopy (ARUPS),[8] but also by EELS (Ref. 9) and optical reflectivity measurements.[10,11] Our distinction between image-potential SS's and intrinsic SS's corresponds to *barrier-induced* and *crystal-induced states,* respectively, in the notation of Echenique and Pendry.[12] In contrast, extrinsic SS's are due to defects, irregularities, steps, etc., at the surface.

Here, we present KRIPES results for the Ag(100) surface which offers the unique possibility to study image potential *and* intrinsic SS's under identical conditions, since they are existent on the same surface. Similar as for the Ag(110) surface,[1] the intrinsic surface states on Ag(100) were calculated using self-consistent pseudopotential calculations and found in agreement with electroreflectance measurements[11] which place it at $E_F+3.3$ eV. Our results give a value of $E_F+(3.8\pm0.4)$ eV for the SS at the $\bar{X}$ point of the surface Brillouin zone (SBZ), which corresponds to the bulk *L* point.[13] In addition, we now present the band dispersion along $\bar{\Gamma}\bar{X}$ and $\bar{X}\bar{M}$ for the intrinsic SS, and along $\bar{\Gamma}\bar{X}$ for the image-potential state as well as their behaviors when Ag(100) is exposed to water vapor at 110 K.

The experiments were performed in an ultrahigh-vacuum vessel with a base pressure in the 10^{-11}-Torr range, which was equipped with LEED and Auger electron spectroscopy (AES). The Ag(100) specimen was mechanically and chemically polished until it exhibited a mirrorlike finish, and then inserted into the vacuum through an interlock system. Repeated cycles of 1-kV Ne^+-ion bombardment and annealing at $\sim 700\,^{\circ}C$ produced an atomically clean (as checked by AES) and well-ordered surface with a $p(1\times1)$ LEED pattern. The sample could be cooled to 110 ± 10 K as monitored by a thermocouple. Triply distilled water was used for the low-temperature adsorption experiments.

KRIPES measurements were performed by bombarding the sample with electrons from a custom-made gun equipped with a BaO cathode,[14] and monitoring the intensity of the outcoming photons at $h\nu=9.7$ eV and mixed *s,p* polarization with a Geiger-Müller-type counter[14,15] as a function of electron energy. The overall resolution (electrons and photons) was 0.7 eV.[14] The azimuthal orientation of the SBZ with respect to the incident electron beam was set with the help of the LEED pattern. Normal incidence (polar angle $\theta=0$) was determined from the minimum of the dispersion of the major peak near E_F for positive and negative θ. The divergence of the incident electron beam was estimated to be $\Delta\theta=10°$ which resulted in an uncertainty of $k_{\parallel}$, the wave vector parallel to the surface, of $\Delta k_{\parallel}=0.15$ Å^{-1}.

KRIPES spectra from Ag(100) measured along the symmetry line $\bar{\Gamma}\bar{X}$ of the SBZ are presented in Fig. 1. The normal-incidence ($k_{\parallel}=0$) curve is dominated by a sharp and intense emission feature at E_F, which has also been observed for isoelectronic Cu(100) (Refs. 2 and 3) and can be attributed to a direct optical transition between the bulk bands 7 and 6 of Δ_6 symmetry.[16] The asymmetric shoulder around $E_F+1.5$ eV arises from bulk transitions between band 8 and band 6 which disperses to higher energies near the bulk *X* point. In going away from normal incidence along the bulk [110] direction, bulk bands within the plane given by ΓXKL are sampled, which are projected onto the surface $\bar{\Gamma}\bar{X}$ line. Optical transitions from bands 7, 8, and 9 into the final-state band 6 account for the intense emission feature which moves away from E_F. This is similar as for Cu(100) for which KRIPES data could be very well explained within the two-band approximation.[17]

The interesting features and main subjects of this Rapid Communication are the structures in Fig. 1 at higher energies (~4 eV), which we have dotted in the case of the image-potential SS, and dashed in the case of the intrinsic SS. In the normal-incidence spectrum, the maximum of the

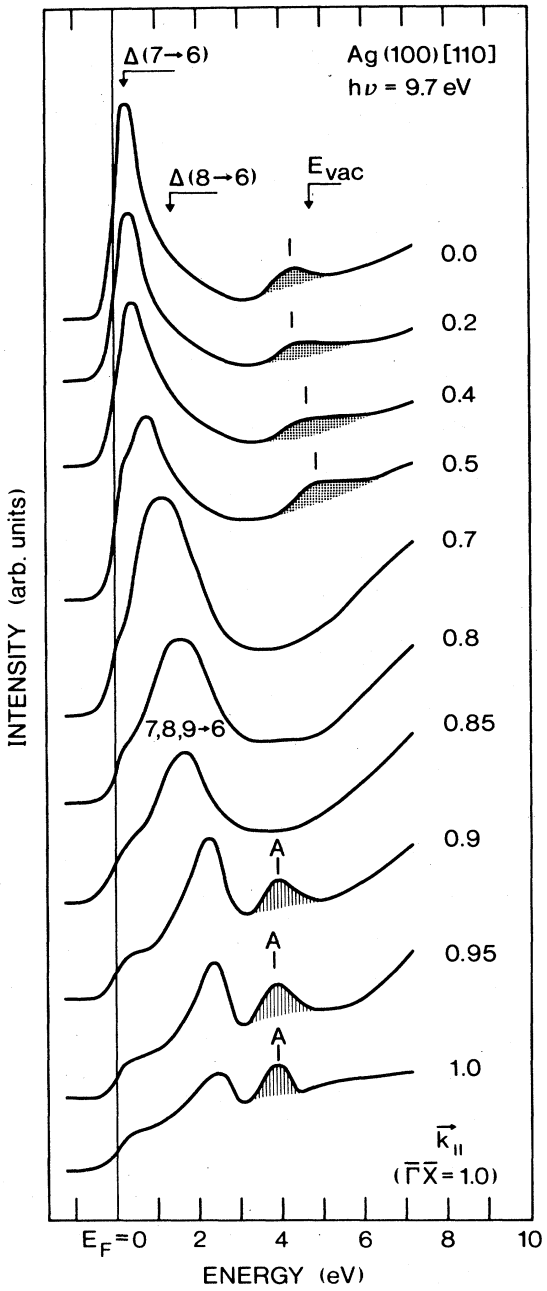

FIG. 1. $\vec{k}$-resolved inverse photoemission spectra at $h\nu = 9.7$ eV from Ag(100) as a function of $\vec{k}_{\parallel}$ along the $\bar{\Gamma}\bar{X}$ azimuth. The $k_{\parallel}$ values belong to an energy of 4 eV, which is about the position of the image-potential SS features (dotted) and intrinsic SS features A (shaded). $k_{\parallel} = 1.0\bar{\Gamma}\bar{X} = 1.09$ Å^{-1} corresponds to a polar angle $\theta = 45°$ [see, e.g., Ref. 17 for the $k_{\parallel}(\theta)$ relationship]. Direct bulk transitions $\Delta(7 \rightarrow 6)$, $\Delta(8 \rightarrow 6)$, and $(7,8,9 \rightarrow 6)$ are indicated (cf. Ref. 16). Also shown is $E_{vac} = 4.64$ eV (from Ref. 18).

image-potential feature is 0.5(5) eV below $E_{vac} = E_F + \phi = 4.64$ eV,[18] which is consistent with the 0.6 eV found for the isoelectronic Cu(100) (Refs. 2–5) and the reconstructed Au(100)-(5×20) (Ref. 5) surfaces. For the transition-metal surface Ni(100), a markedly higher value of 0.9 eV has been found.[2] Despite the universal character of the image-potential state, the coupling of its wave function to the bulk seems to depend on the surface electronic structure, and hence determines its energetic position with respect to E_{vac}.

In principle, the dotted spectral features in Fig. 1 consist[12] of a Rydberg series of states with energies $E_n = \hbar^2 k_{\parallel}^2 / 2m^* - c/n^2 + E_{vac}$, where m^* is the effective electron mass, $c = \text{const}$, $n = 1, 2, 3, \ldots$, but the lifetime broadening and our limited energy resolution do not allow the distinct n contributions to be resolved. Instead, in Fig. 1 we observe the parabolic dispersion of the Rydberg series as a whole towards higher energies. (Also note its increasing width with increasing $k_{\parallel}$.) In Fig. 2, the calculated bulk-band structure projected onto the SBZ[11] is displayed. We note the energy gap above 2 eV at $\bar{\Gamma}$, into which the image-potential SS's fall. The open dots denote the positions of the maxima from Fig. 1. The solid line through these dots represents the fit by a parabola with $m^* = (1.6 \pm 0.3)m$ according to the above formula (m is the free-electron mass). This effective mass for the image-potential SS band on Ag(100) is somewhat higher than the $m^* = (1.2 \pm 0.2)m$ found for Cu(100) (Ref. 4) indicating a reduced dispersion of the image-potential SS band on Ag(100) as compared to Cu(100). Presumably, this goes along with the decreasing width of the gap at $\bar{\Gamma}$ given by $X_6^+ - X_6^-$ in going from Cu (5.1 eV) to Ag (4.5 eV) to Au (4.1 eV).[16] The specific influence of the bulk electronic structure on the image-potential SS again accounts for these distinctive differences, likewise for their energetic positions discussed above. (See note added in proof.)

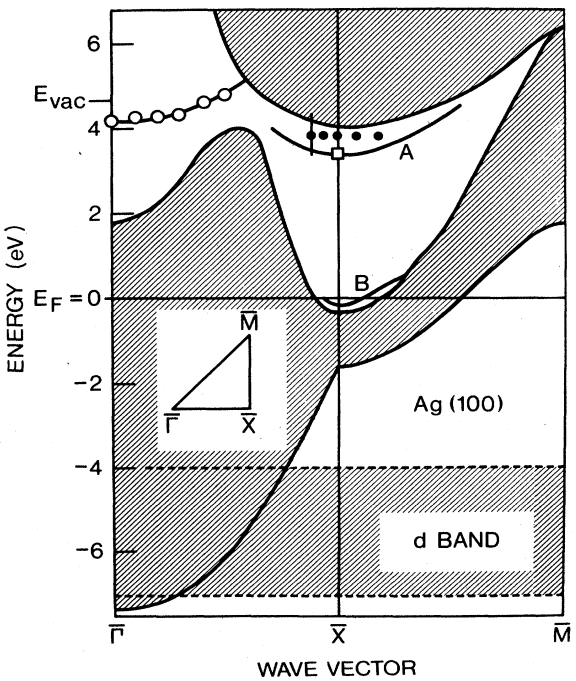

FIG. 2. The calculated electronic-band structure of Ag projected onto the (100) SBZ (shaded area) and the predicted surface-state bands A and B (solid lines) around the $\bar{X}$ point after Kolb and coworkers (Ref. 11). The electroreflectance data from Ref. 11 is given by the open square. Our data for the intrinsic SS band are given by full dots. The vertical bar represents the full width at half maximum of the SS peak in Fig. 1. Our data for the image-potential SS band are shown by open circles. The connecting solid line represents a parabolic fit with $m^* = 1.6m$ (see text).

Owing to the long-range nature of the image potential, the corresponding SS's are spatially concentrated far from the surface.[12] Therefore, the local-density pseudopotential calculations of Kolb, Boeck, Ho, and Liu[11] cannot be expected to yield the image-potential SS's, instead they predict intrinsic SS bands near $\bar{X}$ of the SBZ denoted A and B (cf. Fig. 2), which are spatially located right at the surface-vacuum interface. The SS band B is partially occupied. Both SS's A and B have been observed in electroreflectance measurements,[11] where the Ag(100) sits in an electrolyte solution. The nonobservation of the image-potential state in electroreflectance is probably caused by the extremely low overlap of the bulklike initial-state wave function with the image-potential wave function outside the crystal.[12] With KRIPES, we see an emission feature appearing at $E_F+(3.8\pm0.4)$ eV when $\vec{k}_{\parallel}$ approaches the $\bar{X}$ point (see Fig. 1). As with the image-potential states, this feature is very sensitive to oxygen or water adsorption (to be discussed below) and we associate the SS band A therewith. In Fig. 2, we have plotted the experimentally derived energy dispersions along $\bar{\Gamma}\bar{X}$ as well as $\bar{X}\bar{M}$. The latter was obtained from KRIPES spectra (not shown) which we took to search for the unoccupied part of the SS band B. Probably owing to its proximity ($\sim$0.1 eV) to projected bulk bands (cf. Fig. 2) and our limited energy resolution, we did not find any evidence for B in our spectra. Only on Au(100) (Ref. 19) and Cu(100) (Ref. 20) has the occupied part of B been found close to E_F using ARUPS. Finally, we note that as with the s-like SS band on Ag(110) (Ref. 1) the energy position of A on Ag(100) is larger (by $\sim$0.6 eV) than the calculated SS band and, furthermore, that the width of the emission feature A in Fig. 1 has its minimum (0.9 eV) at $\bar{X}$, which is $\sim$0.1 eV more than on Ag(110). This observation indicates an increased lifetime broadening when the SS band is closer to [Ag(100) vs Ag(110)] or approaches the projected bulk bands, therewith becoming more a surface resonance. Our nonobservation of the SS band B may also be due to this effect.

A necessary condition to be fulfilled by surface states is their sensitivity to gas adsorption. This has been greatly exploited for occupied SS's using ARUPS.[8] The unoccupied SS on Ag(110) could also be quenched by exposing the surface to about 1 langmuir (1 L$=10^{-6}$ Torr sec) of activated hydrogen or oxygen.[1] In the case of Ag(100) discussed here, about 200 L of activated oxygen were necessary to quench the intrinsic SS feature A and also the image-potential SS. The geater amount of gas adsorption is due to the increased inertness of the close-packed Ag(100) surface as compared to Ag(110). Here, in Fig. 3, we have chosen to present the behavior of the surface states when H_2O is adsorbed onto the surface at 110 $\pm$10 K. Below $T=170$ K, water is known to adsorb on Ag(100) as a molecule with a sticking coefficient close to one.[21] In contrast to activated oxygen, the interaction of H_2O with the Ag surface is small.

In view of the above-mentioned differences between the image-potential and intrinsic surface states, we would have expected a different behavior of the SS's with adsorption: A redistribution of charge would mainly influence the electrons near E_F and result in a change of the surface electronic structure. This should preponderantly alter the intrinsic SS, while the image-potential state located further away from the surface should be less affected, except for a shift in absolute energy, if the adsorption changed the work function ϕ and therewith E_{vac}. On the other hand, image-potential SS's may be more sensitive to changes of the dielectric properties at the surface.[12] Inspection of Fig. 3, however, reveals that both surface states are simultaneously quenched by the exposure of 0.4 L H_2O. In contrast to the reported shift of the image-potential state on Cu(100) after Cl exposure,[4] we do not see a shift of the image-potential SS nor of the intrinsic SS. Qualitatively, the quenching of both SS's with H_2O is similar to their behavior with oxygen adsorption on Ag(100) and Ag(110).[1] Although this observation proves the surface origin of both emission features, it is unexpected to find no differences at all between the two states with respect to their behavior under gas adsorption. Species with even a smaller interaction potential than water, e.g., noble gases, will hopefully reveal these differences. Such work is currently in progress in our Laboratory.

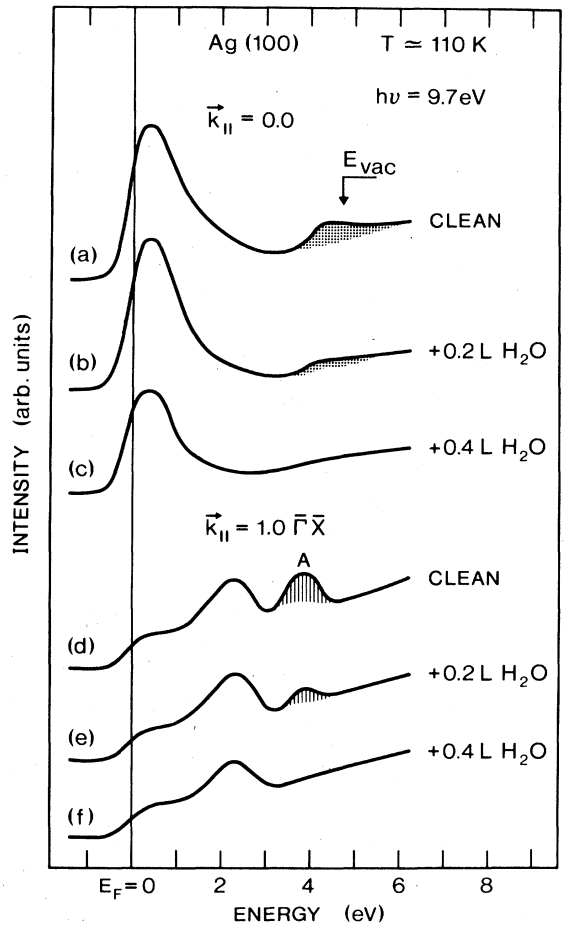

FIG. 3. The adsorption of water on Ag(100) at $T=110\pm10$ K. KRIPES spectra for the clean surface at (a) $\vec{k}=0$ ($\theta=0°$), and (d) $\vec{k}=1.0\bar{\Gamma}\bar{X}$ ($\theta=45°$); (b) and (e), respectively, after adsorption of 0.2 L H_2O; (c) and (f), respectively, after adsorption of 0.4 L H_2O. Note the simultaneous disappearance of the image-potential SS (dotted) and intrinsic SS (dashed) with H_2O adsorption.

Note added in proof. In a new theory N. Garcia *et al.*[22] show the energy position and effective mass of the image states depend on the surface corrugation.

We thank A. Baratoff for stimulating and helpful discussions, H. Neff for his help with the water experiment, and D. Schmid for technical assistance.

[1]B. Reihl, R. R. Schlittler, and H. Neff, Phys. Rev. Lett. **52**, 1826 (1984).
[2]P. D. Johnson and N. V. Smith, Phys. Rev. B **27**, 2527 (1983).
[3]W. Altmann, V. Dose, A. Goldmann, U. Kolac, and J. Rogozik, Phys. Rev. B **29**, 3015 (1984).
[4]V. Dose, W. Altmann, A. Goldmann, U. Kolac, and J. Rogozik, Phys. Rev. Lett. **52**, 1919 (1984).
[5]D. Straub and F. J. Himpsel, Phys. Rev. Lett. **52**, 1922 (1984).
[6]For a review, see E. G. McRae, Rev. Mod. Phys. **51**, 541 (1979).
[7]W. Shockley, Phys. Rev. **56**, 317 (1939).
[8]Here are a few examples for occupied surface states observed by ARUPS. W(100), B. Feuerbacher and B. Fitton, Phys. Rev. Lett. **30**, 923 (1973); Cu(111), P. O. Gartland and B. J. Slagsvold, Phys. Rev. B **12**, 4047 (1975); Ag(111), H. F. Roloff and H. Neddermeyer, Solid State Commun. **21**, 561 (1977); Ni(111), F. J. Himpsel and D. E. Eastman, Phys. Rev. Lett. **41**, 507 (1978).
[9]See, e.g., J. E. Demuth, B. N. J. Persson, and A. J. Schell-Sorokin, Phys. Rev. Lett. **51**, 2214 (1983).
[10]See, e.g., G. Chiarotti, S. Nannarone, R. Pastore, and P. Chiaradia, Phys. Rev. B **4**, 3398 (1971); P. Chiaradia, A. Cricenti, S. Selci, and G. Chiarotti, Phys. Rev. Lett. **52**, 1145 (1984).
[11]D. M. Kolb, W. Boeck, K. M. Ho, and S. H. Liu, Phys. Rev. Lett. **47**, 1921 (1981).
[12]P. M. Echenique and J. B. Pendry, J. Phys. C **11**, 2065 (1978).
[13]See H. J. Levinson, F. Greuter, and E. W. Plummer, Phys. Rev. B **27**, 727 (1983), for a projection of the bulk fcc Brillouin zone onto its (100) surface.
[14]B. Reihl and R. R. Schlittler, Phys. Rev. B **29**, 2267 (1984); E. Haupt, B. Reihl, and R. R. Schlittler, IBM Tech. Disclosure Bull. **26**, 6383 (1984).
[15]V. Dose, Appl. Phys. **14** 117 (1977); V. Dose, Prog. Surf. Sci. **13**, 225 (1983).
[16]H. Eckardt, L. Fritsche, and J. Noffke, J. Phys. F **14**, 97 (1984).
[17]D. P. Woodruff, N. V. Smith, P. D. Johnson, and W. A. Royer, Phys. Rev. B **26**, 2943 (1982).
[18]We take the work function $\phi = 4.64$ eV of Ag(100) as measured by A. W. Dweydari and C. H. B. Mee, Phys. Status Solidi (a) **27**, 223 (1975), using the photo-electric method. The average of existing literature values is 4.63 ± 0.24 eV. The error gives the standard deviation. See the compilation by M. Chelvayohan and C. H. B. Mee, J. Phys. C **15**, 2305 (1982).
[19]P. Heimann, H. Miosga, and H. Neddermeyer, Phys. Rev. Lett. **42**, 801 (1979).
[20]S. D. Kevan, Phys. Rev. B **28**, 2268 (1983). We thank N. V. Smith for pointing out this reference to us.
[21]M. Klaua and T. E. Madey, Surf. Sci. **136**, L42 (1984).
[22]N. Garcia *et al.* (to be published).